量子色力学類似有効理論に於けるクォーク星

木内 一佳志

了徳寺大学・健康科学部医学教育センター

要旨

量子色力学類似有効モデルを用い, コンパクト星拘束条件下に於ける2フレーバーカラー超伝導体のクーパー対の空間構造と本モデルから導かれるクォーク星について調べた. クーパー対のコヒーレンス長は, 概ね1.1fmであった. クォーク化学ポテンシャルが0.4 GeV以下では, コヒーレンス長が平均粒子間距離より短くボゾン的であった. この結果は, クォーク星内部にボース・アインシュタイン凝縮相の存在可能性を示している. 本モデルから算出されるクォーク星の質量と半径は, 導入するバッグ定数(B)に依存する.145 MeV $< B^{\frac{1}{4}} <$ 167MeVの範囲では, 質量は太陽の1.5倍から2倍, 半径は9kmから11kmであった.

キーワード: 量子色力学類似有効モデル, コンパクト星拘束条件, ボース・アインシュタイン凝縮, クォーク星

Quark stars in a QCD-like Effective Theory

Hiyoshi Kiuchi

Faculty of Health Science, Ryotokuji University

abstract

The spatial structure of quark Cooper pairs in two-flavor quark matter is investigated numerically within the framework of a modified QCD-like effective model, in which the lattice-QCD-based gluon propagator is used. The propagator is considered to include the nonperturbative effects in the quenched QCD. We consider β-equilibrated quark matter with electric charge neutrality condition. We find that the coherence length $\xi \sim 1.1\ fm$ at low to moderate quark chemical potential ($0.2 < \mu < 0.7$ GeV). Cooper pair is considered to be bosonic at $\mu < 0.4$ GeV, because $\xi/d < 1$ in the region(d: interquark distance). Therefore, in the universe, the quark-Bose-Einstein condensation may exist inside some of compact stars.

Furthermore, we investigate quark stars in our model. We find that, for example, at $B^{\frac{1}{4}}$=150MeV, the maximum mass is $1.92M_{sun}$ and its radius is $10.61km$ (M_{sun} : solar mass, B : bag constant).

Key words: QCD-like model, compact star constraints, Bose-Einstein condensation, quark star

I. Introduction

A lot of studies on the phase structure of the quantum chromodynamics (QCD) demonstrate that, at sufficiently high temperature (T) and/or quark chemical potential (μ), a system with quarks and gluons make a phase transition from confinement phase (hadronic matter) to deconfinement one (quark-gluon plasma or color superconductor).[1)−12)] The recent progress in mapping the QCD phase diagram has revealed that the deconfinement phase at

low temperature has a rich phase structure including two-flavor color superconducting (2SC) phase and clor-flavor locking (CFL) phase.[13),14)] In the universe, we may expect that such quark matters exist inside compact stars.[15)−17)] Quark matter inside a compact star should be neutral with respect to electric as well as color charges. Especially, electric charge neutrality is essential to hold the star together by the gravitational force.[16),17)]

Some physicists claimed that, under charge neutrality condition, there will be no 2SC phase. In the study, they adopted the framework of the bag model, in which the strange quark mass was very small and the value of the diquark energy gap was arbitrarily determined.[18)]

However, in some studies, it was found that 2SC phase exists even under compact star constraints.[18)−20)] Furthermore, it is shown that the charge neutral 2SC phase is a stable state.[21)] Later, even one of the authors in ref. 22) have discussed the possibility of energetically stable flux tube within the 2SC core region in neutron star.[22)]

For compact stars, relevant baryon chemical potential ($\mu_B = 3\mu$) lies in low to intermediate region ($\mu < 0.5$ GeV, the density might be as large as $10\rho_0$ where $\rho_0 \sim 0.46$ fm^{-3}).[16)] At high-μ region, strangeness is indispensable. However, as the value of μ decreases, strangeness becomes more unimportant. Accordingly, at low to moderate μ region, especially near the deconfining point, quark matter may lie in a 2SC phase that is made up with only up and down quarks.

In cold quark matter, if quark-quark interaction is strong enough, the quarks of a Cooper pair (quark-quark pair) may exist close to each other, in consequence, Cooper pairs may be in Bose-Einstein condensation (BEC). In BEC phase, coherence length (ξ), which is the squared mean distance of two paired particles, is smaller than the averaged interparticle distance (d) of relevant particles ($\xi/d < 1$). Because of the asymptotic freedom of QCD, quark-quark coupling strength subsides as μ grows. Accordingly, realizability of quark-BEC increases as μ decreases. Therefore, the vicinity of the deconfining point is the most probable area for the quark BEC. Recently, some studies have been reported concerning ξ and spatial structure of quark Cooper pairs in 2SC based on the Schwinger-Dyson equation (S-D eq.). In these studies, the tree-level gluon propagator is used. This simplification may result in ignoring possible nonperturbative effects. It is shown in Ref. 9) that the S-D eq. for the effective mass in the ladder approximation can be derived from the QCD-like theory with the tree-level gluon propagator, which is the usual choice in the theory. We can also show that the S-D eq. for diquark energy gap in the ladder approximation can be derived from the same theory. In the QCD-like theory, the one-loop running coupling ($\bar{g}$) is introduced instead of the coupling constant (g) for the quark-gluon vertex. By this improvement, the asymptotic freedom of QCD is satisfied.

The main purpose of the present study is to investigate possibility of the quark-BEC inside a compact star. Electric charge neutrality is imposed for β-equilibrated quark matter. We make use of the lattice-QCD-based gluon propagator instead of the tree-level one in the 3-momentum space, investigation of the ξ in 2SC under compact star constraints (i.e., charge neutrality and $\beta-$equilibrium) within the framework of the QCD-like gauge field theory in the mean-field approximation. The lattice-QCD-based gluon propagator, which is extracted from the lattice QCD data, exhibits the infrared vanishing and strong enhancement at the intermediate-energy region $p \sim 1$ GeV. The propagator is considered to include the nonperturbative effects in the quenched QCD. The intermediate energy region is demonstrated to be the most important region for dynamical chiral symmetry breaking. Throughout the paper, we restrict ourselves to $N_f = 2$, corresponding to a system of up and down quarks. The q-q interaction is most attractive in the Lorentz scalar, total spin singlet ($J = 0$), color anti-triplet ($\bar{3}$) and, therefore, flavor anti-symmetric channel. Consequently, nonzero

diquark condensate $\langle qC\gamma_5 q\rangle$ breaks color $SU(3)$ symmetry down to $SU(2)$ symmetry. Color symmetry breaking as well as dynamical chiral symmetry breaking are nonperturbative phenomena in QCD. Therefore, assuming that the same gluon propagator works for not only $\bar{q}$-q interaction in the CSB phase but also q-q interaction in the chirally symmetric phase, we attempt to combine the QCD-like theory and the lattice-QCD-based gluon propagator for the investigation.

The outline of the paper is as follows. In the next section, we derive the Fierz-rearranged effective Hamiltonian with gluon exchange interaction for two flavors. We combine the lattice-QCD-based gluon propagator with the QCD-like gauge field theory. In §3, we derive a gap equation for momentum-dependent diquark energy gap function $\Delta(\vec{p})$ in the mean-field approximation and the electric charge-neutrality condition for two flavors. In §4, we give the equation for coherence length. In §5, we solve the gap equation and compute Cooper pair wave function and coherence length, and present the numerical results. In §6, we present the equation of state (EoS) of 2SC in our model. In §7, the sequence of quark stars corresponding to the EoS is investigated. Section 8 is devoted to discussions.

II. Effective Hamiltonian

We derive here the Fierz-rearranged effective Hamiltonian with lattice-QCD-based gluon propagator. The effective Hamiltonian (H) that we start with is[23],

$$H = H_0 + H_I, \tag{1}$$

where

$$H_0 = \int d^3x \overline{\Psi}(x)(i\nabla\!\!\!/ - \mu\gamma_0 - m)\Psi(x), \tag{2}$$

$$H_I = \frac{1}{4}\int d^3x d^3y \frac{g^2}{2}\overline{\Psi}(x)\gamma_\mu\frac{\lambda^A}{2}\Psi(x)D(x-y)\overline{\Psi}(y)\gamma^\mu\frac{\lambda^A}{2}\Psi(y), \tag{3}$$

with current quark mass m, the coupling constant g^2 and the color $SU(3)$ matrices λ^A. Here, the gluon propagator $D(x-y)$ is given by

$$D(x-y) = \int \frac{d^3p}{(2\pi)^3}\frac{d(p^2)}{p^2}\mathrm{e}^{-ip(x-y)}, \tag{4}$$

where $d(p^2)$ is the polarization factor.

In this study, for the polarization factor, we adopt that of the lattice-QCD-based gluon propagator which is derived using the quenched lattice QCD data.

The polarization factor $d(p^2)$ is well described by the following analytic function[24),25)]:

$$d(p^2) = Z_g\frac{p^4 + ap^2}{p^4 + \alpha p^2 + \beta}, \tag{5}$$

where $p \equiv |\mathbf{p}|$, $a = 7.887$ GeV^2, $\alpha = 1.254$ GeV^2, $\beta = 0.7175$ GeV^4 and $Z_g = 0.7172$.

In this study, we concentrate on the Lorentz scalar $qC\gamma_5 q(\bar{q}C^\dagger\gamma_5\bar{q})$ bilinears in two-flavor quark matter. In $2SC$ phase, a nonzero diquark condensate consists of only two of the three colors.

We assume that the most important interactions are those involving Cooper pairs that

have the lowest energy. Therefore, we select zero-momentum Cooper pairs. Performing Fierz-rearrangement and then dropping all other interactions, the relevant Hamiltonian becomes

$$\hat{H} = \hat{H}_0 + \hat{H}_I \tag{6}$$

where

$$\hat{H}_0 \equiv \sum_{\mathbf{p}} (e_{\mathbf{p}} - \mu) C_R^{\dagger\alpha,s}(\mathbf{p}) C_R^{\alpha,s}(\mathbf{p}) + R \to L \tag{7}$$

$$\begin{aligned} \hat{H}_I \equiv & -\frac{1}{12} g'^2 \sum_{\mathbf{p},\mathbf{p}'} D(\mathbf{p},\mathbf{p}') C_R^{\alpha,s\dagger}(\mathbf{p}) C_R^{\beta,t\dagger}(-\mathbf{p}) C_R^{\gamma,i}(-\mathbf{p}') C_R^{\delta,j}(\mathbf{p}') \\ & \times \epsilon_{\alpha\beta 3}\epsilon_{\gamma\delta 3}\epsilon_{st}\epsilon_{ij} \\ & + R \to L, \end{aligned} \tag{8}$$

where

$$D(\mathbf{p},\mathbf{p}') = \frac{d(|\mathbf{p}-\mathbf{p}'|^2)}{|\mathbf{p}-\mathbf{p}'|^2}. \tag{9}$$

Here $C_{R(L)}^{\dagger\alpha,s}/C_{R(L)}^{\alpha,s}$ denotes the creation/annihilation operator of a right(left)-handed particle with color α and flavor s, $e_{\mathbf{p}} \equiv \sqrt{|\mathbf{p}|^2 + m^2}$, $g'^2 = \frac{1}{6}g^2$, $\alpha, \beta, \gamma, \delta$ denote color indices, i, j, s, t denote flavor indices.

We assuse that the Fermi sphere of the quarks bearing the third color is intact. We choose a variational wave function for the ground state $|\Psi_g\rangle$ of the form,

$$\Psi_g = \Psi_L^\dagger \Psi_R^\dagger |0\rangle, \tag{10}$$

where

$$\Psi_R^\dagger = \prod_{s,t,\alpha,\beta,\mathbf{p}} [u_{\mathbf{p}} + v_{\mathbf{p}} C_R^{\dagger\alpha,s}(\mathbf{p}) C_R^{\dagger\beta,t}(-\mathbf{p}) \epsilon_{\alpha\beta 3}\epsilon_{st}], \tag{11}$$

$$\Psi_L^\dagger = R \to L, \tag{12}$$

Here, the color indices α and β run from 1 to 2, and the parameters obey the constraint that

$$u_{\mathbf{p}}^2 + v_{\mathbf{p}}^2 = 1. \tag{13}$$

Then, we find that the diquark condensate is calculated as

$$\langle \Psi_g | C_R^{\dagger\alpha,s}(\mathbf{p}) C_R^{\dagger\beta,t}(-\mathbf{p}) \epsilon_{\alpha\beta 3}\epsilon_{st} | \Psi_g \rangle = (N_c - 1) N_f u_{\mathbf{p}} v_{\mathbf{p}}. \tag{14}$$

Ⅲ. Charge-neutral two-flavor quark matter

In this section, we derive the gap equation in an electrically neutral two-flavor quark matter. It is very likely that color superconducting phase may exist inside some of the compact stars, where the charge neutrality condition should be satisfied. Furthermore, the quark matters inside compact stars need to satisfy the β-equilibrium, that is, β-processes such as ($d \to u + e^- + \overline{\nu}_e$, $u + e^- \to d + \nu_e$) should go with equal rate in opposite direction. As a result, when neutrinos are untrapped, chemical potentials of up quark (μ_u), down quark

(μ_d) and electron (μ_e) satisfy a relation, $\mu_d = \mu_u + \mu_e$. In this study, we introduce only the electric charge neutrality, and ignore the color-charge one.

The net charge of the two-flavor quark matter Q is given by

$$Q = \frac{2}{3}n_u - \frac{1}{3}n_d - n_e. \tag{15}$$

In addition, we note that the particle number densities can be calculated as

$$n_j = -\frac{\partial\Omega}{\partial\mu_j}, \tag{16}$$

where j denotes up quark, down quark and electron.

With these in mind, we set the chemical potentials μ_d, μ_u as follows:

$$\mu_u = \mu - \frac{2}{3}\mu_e, \qquad \mu_d = \mu + \frac{1}{3}\mu_e, \qquad \overline{\mu} = \frac{\mu_u + \mu_d}{2} = \mu - \frac{\mu_e}{6}. \tag{17}$$

Adding only the effect of nonzero diquark condensate on thermodynamic potential at $\mu = \overline{\mu}$ to the thermodynamic potential of noninteracting unpaired quark matter, we obtaine the approximated thermodynamic potential in the charge-neutral system Ω_{CN} as

$$\begin{aligned}
\Omega_{CN} &= \langle\Psi_g|\hat{H} - \mu_u\hat{N}_u - \mu_d\hat{N}_d|\Psi_g\rangle_{\Delta\neq 0} - \langle\Psi_g|\hat{H} - \mu_u\hat{N}_u - \mu_d\hat{N}_d|\Psi_g\rangle_{\Delta=0} \\
&\quad +\Omega_{free} \\
&= 2(N_c-1)\sum_{\mathbf{p}}\left[2(e_{\mathbf{p}} - \overline{\mu})v_{\mathbf{p}}^2 - \Delta_{\mathbf{p}}u_{\mathbf{p}}v_{\mathbf{p}} - \Delta_{\mathbf{p}}u_{\mathbf{p}}v_{\mathbf{p}}\right. \\
&\quad \left. -(e_{\mathbf{p}} - \overline{\mu})\left(1 - \frac{e_{\mathbf{p}} - \overline{\mu}}{\sqrt{(e_{\mathbf{p}} - \overline{\mu})^2}}\right)\right] + \Omega_{free} \\
&= 2(N_c-1)\sum_{\mathbf{p}}\left[(e_{\mathbf{p}} - \overline{\mu})^2\left(\frac{1}{\sqrt{(e_{\mathbf{p}} - \overline{\mu})^2}} - \frac{1}{E_{\mathbf{p}}}\right) - \frac{\Delta_{\mathbf{p}}^2}{E_{\mathbf{p}}}\right] \\
&\quad +\Omega_{free}
\end{aligned} \tag{18}$$

where Ω_{free} is the thermodynamic potential of the free particle system,

$$\Omega_{free} = -\frac{3\mu_u^4 + 3\mu_d^4 + \mu_e^4}{12\pi^2}. \tag{19}$$

and

$$E_{\mathbf{p}} = \sqrt{(e_{\mathbf{p}} - \overline{\mu})^2 + \Delta_{\mathbf{p}}^2}. \tag{20}$$

Here, we introduce the gap function $\Delta_{\mathbf{p}}$:

$$\Delta_{\mathbf{p}} = \frac{1}{2}g'^2\sum_{\mathbf{p}'}D(\mathbf{p},\mathbf{p}')\langle C_{R(L)}(-\mathbf{p}')C_{R(L)}(\mathbf{p}')\rangle \tag{21}$$

$$= (N_c-1)N_f\frac{g'^2}{2}\sum_{\mathbf{p}'}D(\mathbf{p},\mathbf{p}')u_{\mathbf{p}'}v_{\mathbf{p}'}. \tag{22}$$

In addition, we find that

$$\begin{aligned}\langle C_{R(L)}(-\mathbf{p})C_{R(L)}(\mathbf{p})\rangle = u_{\mathbf{p}}v_{\mathbf{p}} &= \frac{\Delta_{\mathbf{p}}}{2E_{\mathbf{p}}} \\ &\equiv \phi(\mathbf{p}).\end{aligned} \tag{23}$$

If the extremum of the thermodynamic potenyial Ω_{CN} is realized by $\Delta_{\mathbf{p}}$, it must satisfy the following stationary condition:

$$\frac{\delta\Omega_{CN}}{\delta\Delta_{\vec{p}}} = 0, \tag{24}$$

which yields the following gap equation

$$\Delta_{\mathbf{p}} = \left[\frac{(N_c-1)N_f}{12}g^2\sum_{\mathbf{p},\mathbf{p}'}D(\mathbf{p},\mathbf{p}')\frac{\Delta_{\mathbf{p}}}{2E_{\mathbf{p}}}\right]_{\mu=\overline{\mu}}. \tag{25}$$

In the QCD-like theory, the one-loop running coupling ($\bar{g}$) is introduced instead of the coupling constant (g) for the quark-gluon vertex with an infrared regularization parametor p_R:

$$g^2 \to \bar{g}^2(p^2) = \frac{2\pi b}{\log[(p^2+p_R^2)/\Lambda_{QCD}^2]}, \tag{26}$$

where

$$b = \frac{6(N_c^2-1)}{2N_c(11-2N_f/3)}. \tag{27}$$

It should be noted that the asymptotic freedom in the deep Euclidean region is satisfied by this running coupling $\bar{g}$.

Then, the gap equation we ought to solve is

$$\begin{aligned}\Delta_p &= \left[\frac{(N_c-1)N_f}{12}\int\frac{dp'}{2\pi^2}\bar{g}^2(p,p')D(p-p')\frac{\Delta_{p'}}{2E_{p'}}\right]_{\mu=\overline{\mu}} \\ &= \left[\int\frac{dp'}{12\pi^2}\cdot\frac{p'^2\Delta_{p'}}{E_{p'}}\cdot\frac{Z_g\bar{g}^2(p,p')[(p-p')^2+a]}{(p-p')^4+\alpha(p-p')^2+\beta}\right]_{\mu=\overline{\mu}},\end{aligned} \tag{28}$$

where $p \equiv |\vec{p}|$.

The electrical charge-neutrality condition is given by

$$\begin{aligned}0 &= \frac{\partial\Omega_{CN}}{\partial\mu_e} \\ &= \frac{(N_c-1)}{3}\sum_{\mathbf{p}}(e_{\mathbf{p}}-\overline{\mu})\left[\frac{2}{\sqrt{(e_{\mathbf{p}}-\overline{\mu})^2}}-\frac{2}{E_{\mathbf{p}}}+\frac{\Delta^2}{E_{\mathbf{p}}^3}+(e_{\mathbf{p}}-\overline{\mu})^2\left(\frac{1}{E_{\mathbf{p}}^3}-\frac{1}{(\sqrt{(e_{\mathbf{p}}-\overline{\mu})^2})^3}\right)\right] \\ &\quad+\frac{2\mu_u^3-\mu_d^3-\mu_e^3}{3\pi^2},\end{aligned} \tag{29}$$

IV. Coherence length ξ

The two-body wave function of a quark Cooper pair apart from unimportant normalization constant $\phi(\mathbf{r})$ is given by

$$\begin{aligned}\phi(\mathbf{r}) &= \int \frac{d^3p}{(2\pi)^3}\phi(\mathbf{p})\mathrm{e}^{-i\mathbf{p}\cdot\mathbf{r}} \\ &= \int_0^\infty \frac{p^2dp}{2\pi^2}\phi(\mathbf{p})j_0(pr),\end{aligned} \tag{30}$$

where $\phi(\mathbf{p}) = \frac{\Delta_\mathbf{p}}{2E_\mathbf{p}}$ and $j_0(pr) = \frac{\sin(pr)}{pr}$ is the zeroth-order spherical Bessel function of the 1st kind with $p = |\mathbf{p}|$ and $r = |\mathbf{r}|$.

The coherence length (ξ), which is defined by the squared mean distance of twopaired particles, can be calculated as

$$\xi = \left(\frac{\int d^3r|\phi(\mathbf{r})|^2r^2}{\int d^3r|\phi(\mathbf{r})|^2}\right)^{\frac{1}{2}}. \tag{31}$$

The averaged interparticle distance (d) of quarks of color 1 and 2 is given by

$$d \sim \rho^{-\frac{1}{3}}, \tag{32}$$

where ρ is the relevant quark density.

V. Spatial structure

In this section, we calculate the coherence length ξ of quark Cooper pairs using the momentum-dependent pair wave function by solving the gap equation. For the numerical calculation, we set the values of Λ_{QCD} and the infrared regulator(p_R) in the running coupling to 220 MeV and $2.207\Lambda_{QCD}$, respectively.

The pair wave functions ϕ in momentum and in co-ordinate spaces are plotted in Fig. 1 and Fig. 2, respectively. As shown in Fig. 1, the pair wave functions in momentum space have finite values at $|\mathbf{p}| = 0$, enhanced at $|\mathbf{p}| \sim \mu$, and then decrease as $|\mathbf{p}|$ grows. While, as shown in Fig. 2, the pair wave functions in co-ordinate space have the maximum values at $|\mathbf{r}| = 0$, and decrease as $|\mathbf{r}|$ grows. In addition, we find that the value of $\phi(\mathbf{r})$ at $|\mathbf{r}| = 0$ increases as μ increases. This means that two quarks in a Cooper pair get close to each other as μ grows.

Figure 3 plots the value of μ_e as a function of μ. The value of μ_e increases monotonically as μ increases.

Figure 4 plots the quark number density ρ as a function of μ. The values of ρ at $\mu = 0.4$ GeV and at $\mu = 0.5$ GeV are $\rho = 3.55\rho_0$ and $\rho = 6.82\rho_0$, respectively (ρ_0: nuclear matter density).

Figure 5 plots the coherence length (ξ) and the averaged interparticle distance of the relevant quarks (d) as functions of quark chemical potential (μ). ξ as well as d decreases monotonically as μ grows. The lines cross at $\mu \sim 0.4$ GeV. The values of ξ at $\mu = 0.4$ GeV and at $\mu = 0.5$ GeV are 1.1 fm and 1.0 fm, respectively.

Figure 6 displays the ratio ξ/d as a function of μ. The ratio increases almost linearly as μ grows ($\xi/d \sim 1.74\mu + 0.342$). At $\mu < 0.4$ GeV, $\xi/d < 1$.

VI. Equation of state

In this section, we display the equation of state of the charge-neutral two-flavor quark matter in the chiral limit on the P (pressure)-E (energy density) plane.

Energy density (E) can be calculated using Ω_{CN} as,

$$\begin{aligned} E &= -P + \mu_j n_j \\ &= \Omega_B - \mu_j \frac{\partial \Omega_B}{\partial \mu_j}, \end{aligned} \tag{33}$$

where j stands for up quark, down quark and electron,
and

$$\Omega_B \equiv \Omega_{CN} + B. \tag{34}$$

Here we introduce the bag constant B.

Figure 7 plots the pressure P of the quark matter as a function of E at $B^{\frac{1}{4}}$=150MeV. We find a linear relation that $E = 2.9P + 3.9B$.

Figure 8 plots P vs μ at $B^{\frac{1}{4}}$=150MeV.

VII. Quark stars

In this section we investigate the sequence of quark stars corresponding to the equation of state (EoS) in this model.

We consider a static, stationary and spherically symmetric perfect fluid for the stellar system. With these conditions, Einstein's field equation yield the Tolman-Oppenheimer-Volkov (TOV) equation for hydrostatic equilibrium in general relativity[16]:

$$-4\pi r^2 dP(r) = \frac{4\pi r^2 dr E(r) M(r)}{r^2} \cdot \frac{\left[1 + \frac{P(r)}{E(r)}\right]\left[1 + \frac{4\pi r^3 P(r)}{M(r)}\right]}{1 - \frac{2M(r)}{r}}, \tag{35}$$

where we denote the pressure at a radius r by $P(r)$, energy density by $E(r)$ and the mass inside a radius r by $M(r)$:

$$M(r) = \int_0^r 4\pi r'^2 E(r') dr'. \tag{36}$$

We integrate the TOV equation according to the EoS shown in Fig. 7 from the center with a given central energy density until the pressure becomes zero. As a result, a unique relationship among the mass, radius and central energy density is obtained.

Figures 9 and 10 show the sequence of quark stars corresponding to the EoS shown in Fig. 7. Figure 9 shows the relation of M/M_{sun} vs central energy density $E(0)$. It is seen that M/M_{sun} increases as $E(0)$ increases. The maximum mass of the sequence is about $1.92M_{sun}$. Figure 10 displays the mass vs radius (R) relation. The radius decreases as the mass increases.

Furthermore, we investigate effect of the bag constant (B) on the maximum mass and the radius. Figure 11 plots the maximum mass as a function of $B^{\frac{1}{4}}$. Figure 12 plots the radius vs $B^{\frac{1}{4}}$. We find that both M_{max} and R monotonically decreases as B increases.

Figure 13 shows the interior structure of a quark star with $E(0)$ = 1140 MeV/fm^3(=

2.0×10^{15} g/cm^3, $\rho = 6.55\rho_0$ at $\mu = 480$ MeV) at $B^{\frac{1}{4}}$=150MeV as an example. The values of $r - 2M(r)$ are positive everywhere inside the quark stars. This quark star has the mass of $M = 1.92M_{sun}$ and the radius of $R = 10.61$ km.

VIII. Numerical results

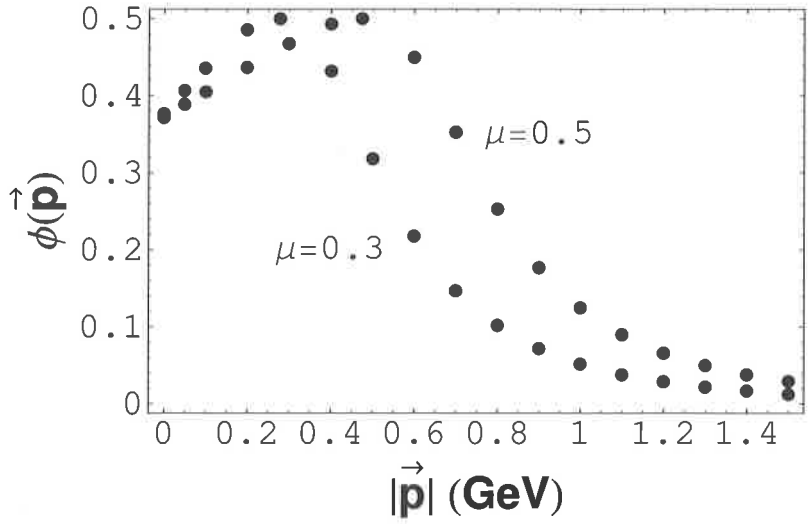

Figure 1: Cooper pair wave functions in momentum space $\phi(\vec{p})$ at $\mu = 0.3$ GeV and at $\mu = 0.5$ GeV.

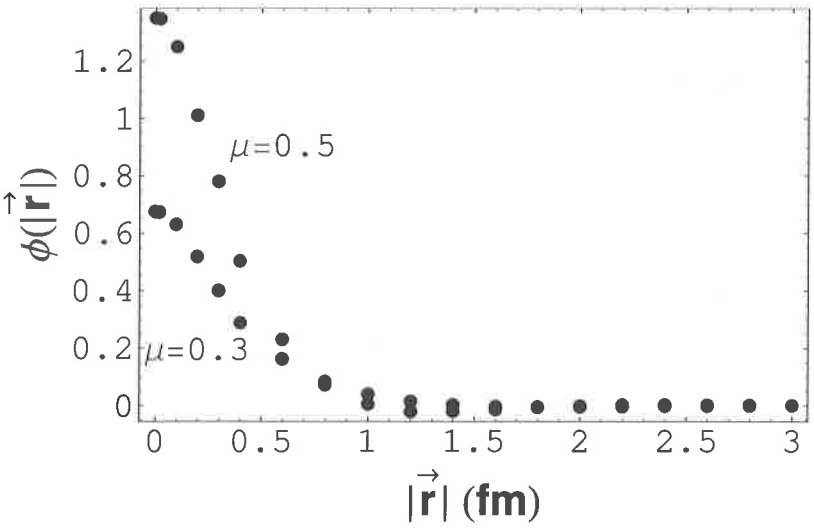

Figure 2: Cooper pair wave functions in co-ordinate space $\phi(\vec{r})$ without normalization constant.

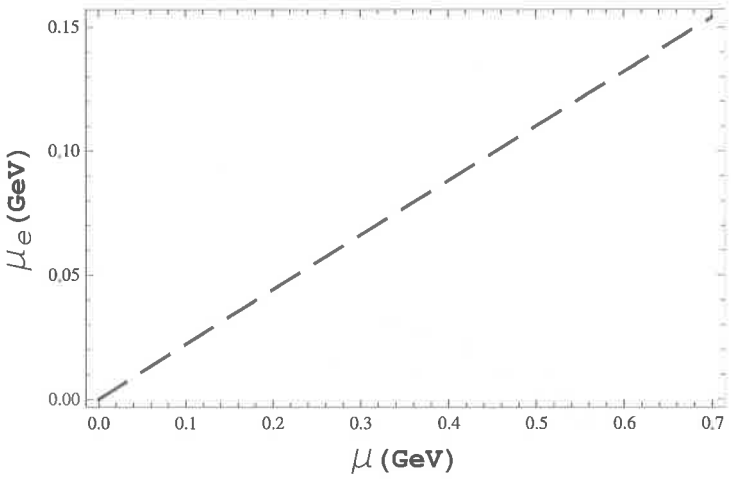

Figure 3: The value of μ_e as a function of μ.

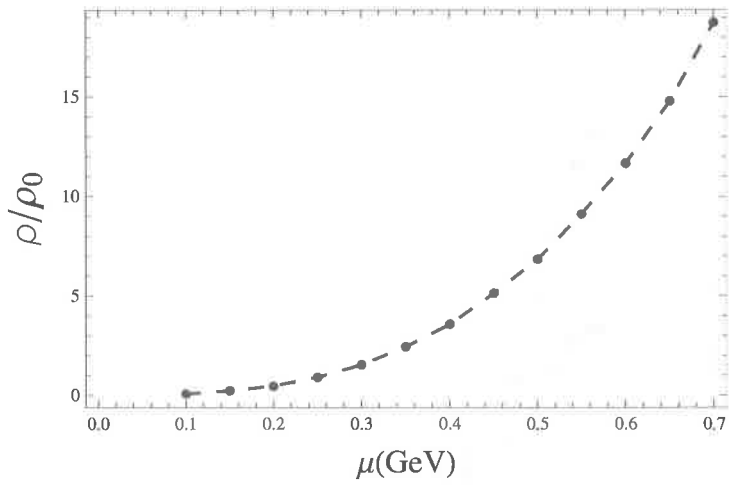

Figure 4: Quark density ρ as a function of μ. The densities at $\mu = 0.4$ GeV and at $\mu = 0.5$ GeV are $\rho = 3.55\rho_0$ and $\rho = 6.82\rho_0$, respectively (ρ_0: nuclear matter density).

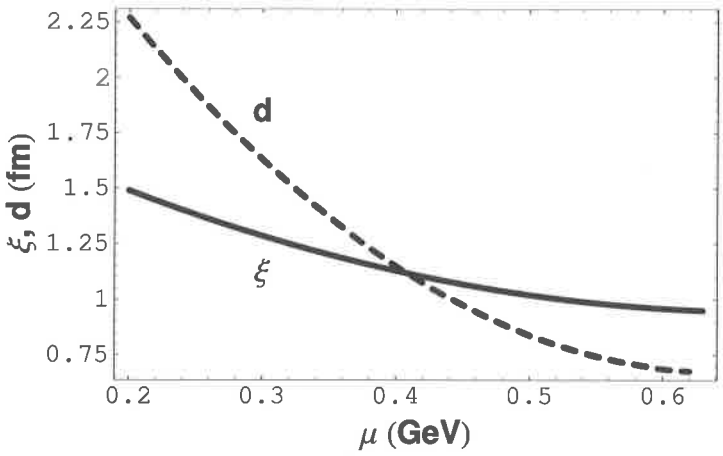

Figure 5: The coherence length (ξ) and the interquark distance (d) as functions of μ. The values of ξ at $\mu = 0.4$ GeV and at $\mu = 0.5$ GeV are 1.1 fm and 1.0 fm, respectively.

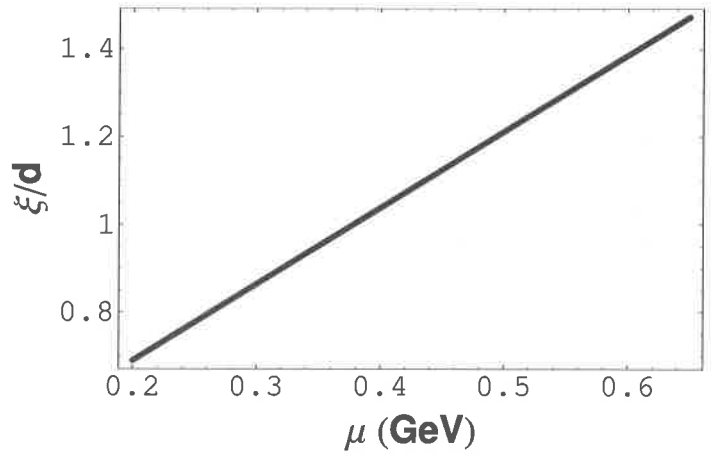

Figure 6: Ratio ξ/d as a function of μ. The ratio ξ/d increases almost linearly as μ grows ($\xi/d \sim 1.74\mu + 0.342$).

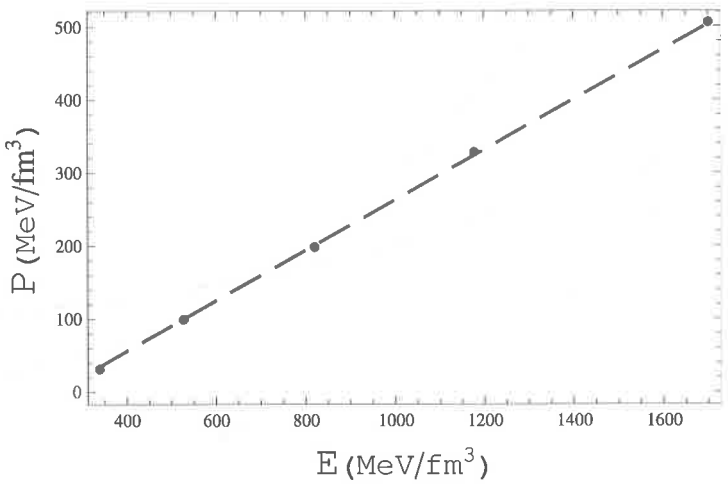

Figure 7: The pressure (P) as a function of the energy density (E) at $B^{\frac{1}{4}} = 150\text{MeV}$.

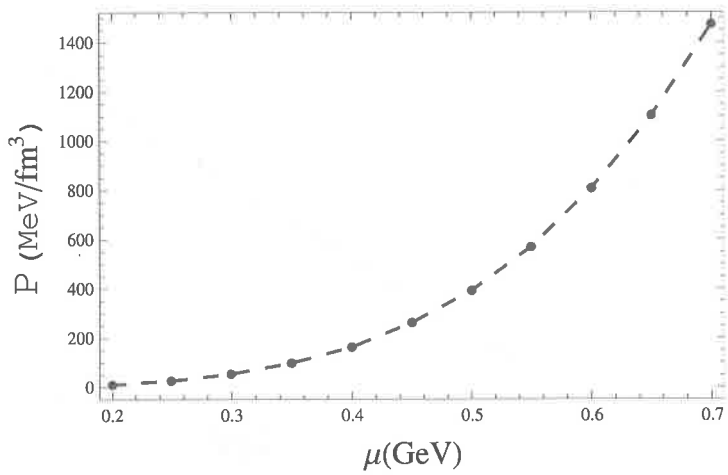

Figure 8: The pressure (P) as a function of the quark chemical potential μ.

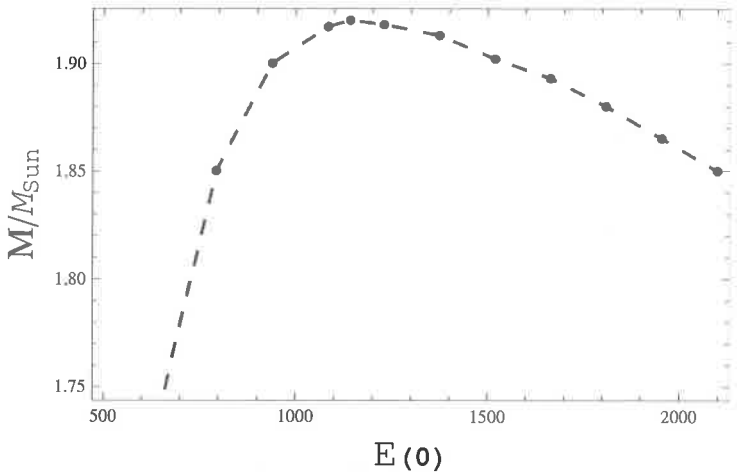

Figure 9: Mass-central energy density relation for quark stars corresponding to the EoS shown in Fig.7.

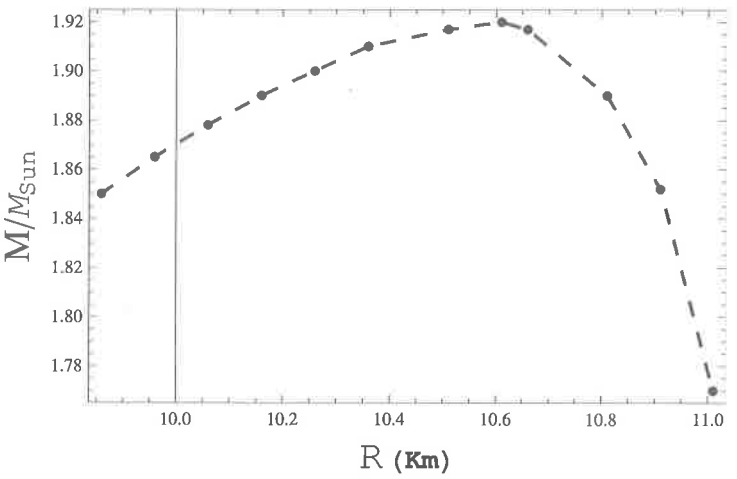

Figure 10: Mass-radius relation for quark stars corresponding to the EoS shown in Fig.7, where $M_{sun} = 1.99 \times 10^{33}\ g$.

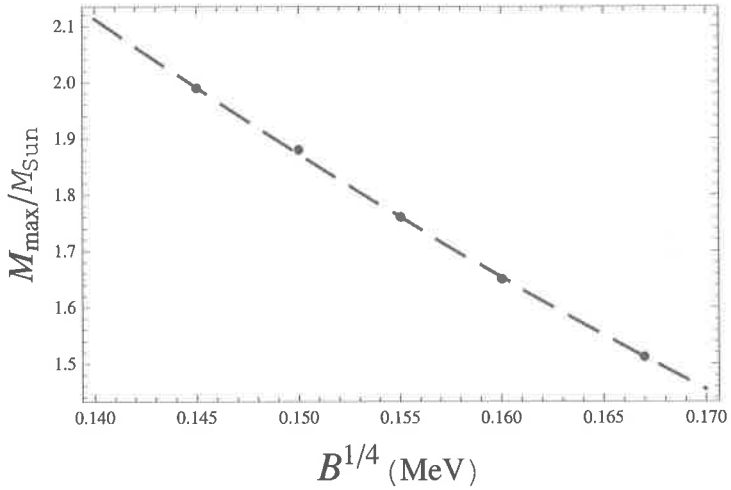

Figure 11: The maximum mass (M_{max}) as a function of the bag constant $B^{\frac{1}{4}}$

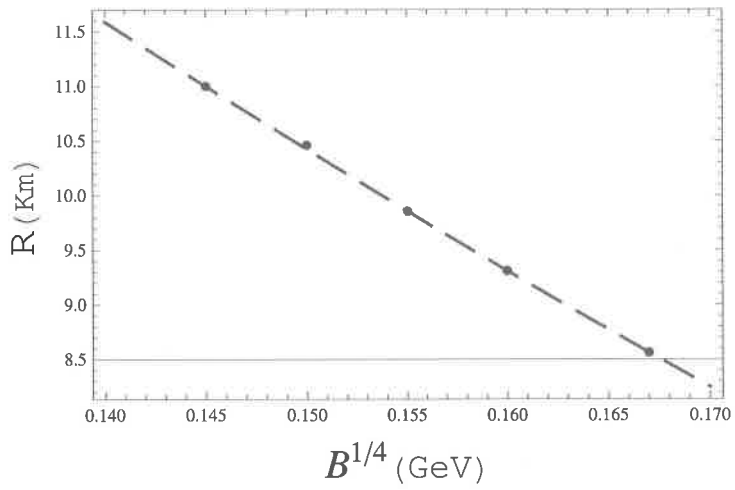

Figure 12: The quark star radius (R) as a function of the bag constant $B^{\frac{1}{4}}$

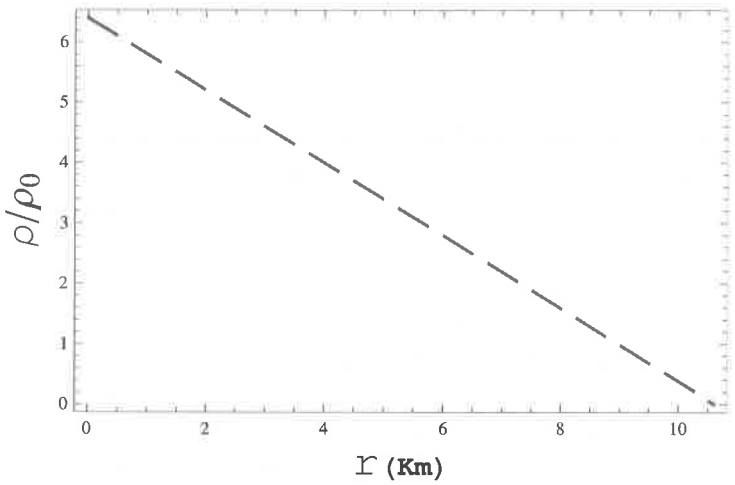

Figure 13: The inner structure of the quark star with $E(0) = 1110$ MeV/fm^3 (2.0×10^{15} g/cm^3). $M = 1.92 M_{sun}$.

IX. Discussions

In this paper, coherence length ξ of quark Cooper pairs in two-flavor quark matter have been investigated under compact star constraints. We have performed this study within the framework of a modified QCD-like theory, in which the lattice-QCD-based gluon propagater which is extracted from the quenched lattice QCD data is used instead of the tree-level one. The lattice-QCD-based gluon propagator is considered to include all the nonperturbative effects in the quenched QCD.

So far a few studies were reported about coherence length ξ of quark Cooper pairs for two flavors. In Ref. 26) and 27), the one-loop Schwinger-Dyson(S-D) equation in the ladder approximation with infrared safe running coupling is used for obtaining Cooper pair wave function. In one of them(Ref.27)), they reported the result only in relatively high density region($\mu > 0.8$ GeV). In the other(Ref.26)),the result in the intermediate density region($0.3 < \mu < 0.65$ GeV) was reported. In addition, we find that the quasiparticle energy in Ref. 26) is that for one-flavor system, because it contain $3\Delta_{\vec{p}}$ $\left(E_{\vec{p}} = \sqrt{(e_{\vec{p}} - \mu)^2 + 3\Delta_{\vec{p}}^2}\right)$ instead of $\Delta_{\vec{p}}$ $\left(E_{\vec{p}} = \sqrt{(e_{\vec{p}} - \mu)^2 + \Delta_{\vec{p}}^2}\right)$. Fortunately, ξ is not affected by the coefficient in front of the gap energy(Δ) in the quasiparticle energy. However, the coefficient affects the magnitude of the gap energy $\Delta_{\vec{p}}$. As mentioned before, it is shown in Ref. 9), that the one-loop S-D eq. with the ladder approximation can be derived from the QCD-like theory with the tree-level gluon propagator.

In the weak-coupling region, which appears in the high density quark matter because of asymptotic freedom of QCD, the coherence length ξ becomes larger than the interquark distance d, while the strong coupling region may appear in low to moderate density quark matter (especially in the vicinity of the deconfining point). For compact stars, relevant baryon chemical potential ($\mu_B = 3\mu$) lies in low to moderate density region ($\mu < 0.4$ GeV, the density might be as large as $10\rho_0$ where $\rho_0 \sim 0.46$ fm^{-3}). The Cooper pair whose ξ is smaller than d suggests that BEC description may be useful as in the analogous example in condensed matter physics.

In our model, we have found the small size Cooper pairs as compared with the interquark distance ($\xi/d < 1$) at $\mu < 0.4$ GeV. Accordingly, the Cooper pairs in the charge-neutral two-flavor quark matter which might exist in the core of compact stars could be rather bosonic and different from that expected from the weak-coupling BCS picture. This situation is similar to the strong-coupling superconductor which could be described by BEC of tightly bound Cooper pairs. Therefore, in the universe, the quark-BEC may exist inside some of the compact stars.

As shown in this study, the averaged chemical potential $\overline{\mu}$ is reduced by $\mu_e/6 > 0$ as $\overline{\mu} \equiv (\mu_u + \mu_d)/2 = \mu - \mu_e/6$. It is found that the repulsive vector interaction has a similar effect.[28] Both reduce the quark chemical potential. The point is that the vector channel interaction ($G_V < \overline{\Psi}\gamma^0\Psi >$) enters the dynamics like the electron chemical poyential μ_e as $\mu_r = \mu - G_V < \overline{\Psi}\gamma^0\Psi >$, where μ_r stands for effective renormalized quark chemical potential, $G_V > 0$ denotes the repulsive vector coupling and $< \overline{\Psi}\gamma^0\Psi >$ is the quark number density. Therefore, when we introduce the electric-charge neutrality and the repulsive vector channel interaction simultaneously, the coherence length will be longer at each μ. Consequently, the value of μ at $\xi = d$ will make an upward shift and, as a result, the region where quark-BEC may exist will be widened.

It should be noted that, in this study, we ignored the $\mu-$dependence of the coupling strength. Therefore, if we use a $\mu-$dependent running coupling, we may obtain more or less different result especialy in relatively high μ region.

The equation of state (EoS) in our model shows a linear relation that $E = 2.9P + 3.9B$, which is similar to that in the MIT bag model. In the bag model, we have $E = 3P + 4B$. However, EoS in our model is slightly stiffer than that in the MIT simple phenomenological bag model.[16] For example, at $B^{\frac{1}{4}}$=150MeV, in the bag model, $P \sim$297 MeV/fm^3 at $E = 1110$ MeV/fm^3. While in our model, $P\sim$308 MeV/fm^3 at $E = 1110$ MeV/fm^3. The bag constant have a large effect on equation of state (EoS) and hence on maximum mass (M_{max}) and radius (R) of quark stars. We have found that both M_{max} and R monotonically decrease as B increases.

We have found that the quark stars in the our model have reasonable relations among masses, radii and central energy densities. The masses are of order M_{sun}, the radii are of order 10 km and the central energy densities are of order 10^{15} g/cm^3. The maximum mass (M_{max}) of the sequence in our model at $B^{\frac{1}{4}}$=150MeV is about $1.92M_{sun}$ and its radius is about 10.6 km. The quark star masses of the sequence in this model are heavier than the typical mass of observed neutron stars, $1.35 \pm 0.04M_{sun}$[29]. However, effects from the strong interaction such as color superconductivity can stiffen the quark matter EoS and increase the maximum mass of a compact star. In fact, a recent estimate of a pulsar mass has shown a possibility of a larger mass. Demorest et al. have estimated the mass of a compact star, which is a millisecond pulsar(PSR J1614-2230)[30]. The estimated pulsar mass of $1.97 \pm 0.04M_{sun}$ is comparable to the M_{max} in the present model.

We expect that we can generalize our model into three-flavor system.

References

1) Asakawa M, Yazaki K (1989) Chiral restoration at finite density and temperature. Nucl Phys. A504, 668-684.

2) Huang M, Zhaung P, Chao W (2002) Massive quark propagator and competition between chiral and diquark condensate. Phys Rev D. 65, 076012-076045.

3) Iwasaki M (2004) First order phase transition in the quark matter. Phys Rev D. 70, 114031-114036.

4) Abuki H, Kitazawa M, Kunihiro T (2005) How do chiral condensates affect color superconducting quark matter under charge neutrality constraints? Phys Lett B. 615, 102-107.

5) Carter GW, Diakonov D (1999) Light quarks in the instanton vacuum at finite baryon density. Phys Rev D. 60, 016004-016014.

6) Kiuchi H, Oka M (2006) Charge neutral two-flavor quark matter in the instanton vacuum and compact stars. Prog Theor Phys. 115, 909-929.

7) Taniguchi Y, Yoshida Y (1997) Chiral symmetry restoration at finite temperature and chemical potential in the improved ladder approximation. Phys Rev D. 55, 2283-2289.

8) Kiriyama O, Maruyama M, Takagi F (2000) Chiral phase transition at high temperature and density in the QCD-like theory. Phys Rev D. 62, 105008-105017.

9) Kiuchi H, Iwasaki M (2004) Latent heat in the chiral phase transition. Prog Theor Phys Suppl. 153, 313-316.

10) Alford M, Rajagopal K, Wilczek F (1998) QCD at finite baryon density; nucleon droplets and color superconductivity. Phys Lett B 42, 247-256.

11) Alford M, Rajagopal K, Wilczek F (1999) Color-flavor locking and chiral symmetry breaking in high density QCD. Nucl Phys B. 537, 443-458.

12) Alford M, Bowers J, Rajagopal K (2001) Crystalline Color Superconductivity. Phys Rev D. 63, 074016-074023.

13) Alford M (2001) Color superconducting quark matter. Ann Rev Nucl Part Sci. 51, 131-160.

14) Alford M (2004) Dense Quark Matter in Nature. Prog Theor Phys Suppl. 153, 1-14.

15) Itoh N (1970) Hydrostatic equilibrium of hypothetical quark stars. Prog Theor Phys. 44, 291-292.

16) Glendenning NK (2000) Compact Stars; Nuclear Physics, Particle Physics and General Relativity, Springer, London. 199-413.

17) Alford M, Rajagopal K (2003) Absence of two-flavor color-superconductivity in compact stars. JHEP. 0206, 031.

18) Huang M, Zhuang P, Chao W (2003) Charge Neutrality Effects on 2-flavor Color Superconductivity. Phys Rev. D 67, 065015-065019.

19) Ruster SB (2004) Effect of color superconductivity on the mass and radius of a quark star. Phys Rev D. 69, 045011-045015.

20) Mishra A, Mishra H (2004) Chiral symmetry breaking, colorsuperconductivity and color neutral quark matter. Phys Rev D. 69, 014014-014019.

21)Shovkovy I, Huang M (2003) Nonstrange hybrid compact stars with color superconduct ing matter. Phys Lett B. 564, 205-210.

22) Alford M, Sedrakian A (2010) Color-magnetic flux tubes in quark matter cores of neutron stars. J Phys G. 37, 075202-075207.

23) Kiuchi H (2012) Thermodynamics of Color Superconductor in a QCD-like effective theory. The Bulletin of Ryotokuji University 5. 11-30.

24) Bowman PO, Heller UM, Leinweber DB et al (2004) Unquenched Gluon Propagator in Landau Gauge. Phys Rev D. 70, 034509-034514.

25) Iida H, Suganuma H, Oka M (2005) Dynamical chiral-symmetry breaking at $T = 0$ and $T \neq 0$ in the Schwinger-Dyson equation with lattice QCD data. Eur Phys J A. 23, 305-315.

26) Matsuzaki M (2000) Spatial structure of quark Cooper pairs in a color superconductor. Phys Rev D. 62, 017501-017504.

27) Abuki H, Hatsuda T, Itakura K (2002) Structural Change of Cooper Pairs and Momentum-dependent Gap in Color Superconductivity. Phys Rev D. 65, 074014-074019.

28) Zhang Z, Kunihiro T (2009) Vector interaction, charge neutrality and multiple chiral critical poin structures. Phys Rev D. 80, 014015-014019.

29) Thorset SE (1999) Neutron star measurements. Radio Pulsars. Astrophys J 512, 288-294.

30) Demorest P (2010) Shapiro delay measurement of a 2 solar mass neutron star. Nature. 467, 1081-1083.

(平成24年11月15日稿)

査読終了年月日　平成24年12月27日